

Hydrological connections in a glaciated Andean catchment under permafrost conditions (33°S)



S. Ruiz Pereira ^{a,b,c}, B. Díez ^{c,d,e}, J. Cifuentes-Anticevic ^d, S. Leray ^{a,f}, F. Fernandoy ^g, C. Marquardt ^h, F. Lambert ^{b,c,*}

^a Departamento de Ingeniería Hidráulica y Ambiental, Pontificia Universidad Católica de Chile, Santiago, Chile

^b Instituto de Geografía, Pontificia Universidad Católica de Chile, Santiago, Chile

^c Center for Climate and Resilience Research, Universidad de Chile, Santiago, Chile

^d Departamento de Genética Molecular y Microbiología, Pontificia Universidad Católica de Chile, Santiago, Chile

^e Millennium Institute Center for Genome Regulation (CGR), Chile

^f Centro de Cambio Global, Pontificia Universidad Católica de Chile, Santiago, Chile

^g Laboratorio de Análisis Isotópico, Universidad Andrés Bello, Viña del Mar, Chile

^h DIEM/DIEG, Escuela de Ingeniería, Pontificia Universidad Católica de Chile, Santiago, Chile

ARTICLE INFO

Keywords:

High Andes
Proglacial aquifer
Mountain permafrost
Transit times
16S rRNA metabarcoding
Cryophilic bacteria

ABSTRACT

Fresh water supply is critical along the Andes, where drought conditions over the past decade are projected to persist. At high Andean headwater catchments, frozen ground conditions are assumed to modulate groundwater flow paths and their hydrological signals at different time-scales. However, knowledge of hydrological connections in subtropical Andean catchments is still very sparse. This study assessed hydrological connections and their impacts on groundwater contribution to baseflow in a headwater proglacial aquifer located in central Chile at 33° S and 3600 m a.s.l. We collected and analyzed snow, glacial stream, and groundwater spring water samples between 2019 and 2021. We combined of water isotope and metagenomic proxies with the hydraulic parameterization of the catchment to deliver mean transit time distributions through the proglacial aquifer. The new hydrological insights for the region include the finding that groundwater spring signals delivered sub-decadal transit times, implying likely origins from glacial or interstitial ice. Additionally, the stable isotope signature showed that groundwater consistently differs from snow and surface runoff. The 16S rRNA metabarcoding analyses demonstrated the presence of psychrophilic microorganisms in groundwater springs, supporting the idea of a late warm-season activation of interstitial ice due to thawing events associated with a differential relative-abundance of specific cryophilic bacteria. Finally, our results suggest hydrological connections and dampening timeframes between glaciers, proglacial areas, and groundwater springs, most likely from thawing sources.

1. Introduction

Millions of people depend on freshwater provided by the mountain cryosphere along the Andean mountain range (Barnett et al., 2005; DeSa, 2013). The Andes mountains between 30° and 38° S have had a declining precipitation trend between 1960 and 2016

* Corresponding author at: Instituto de Geografía, Pontificia Universidad Católica de Chile, Santiago, Chile.

E-mail address: lambert@uc.cl (F. Lambert).

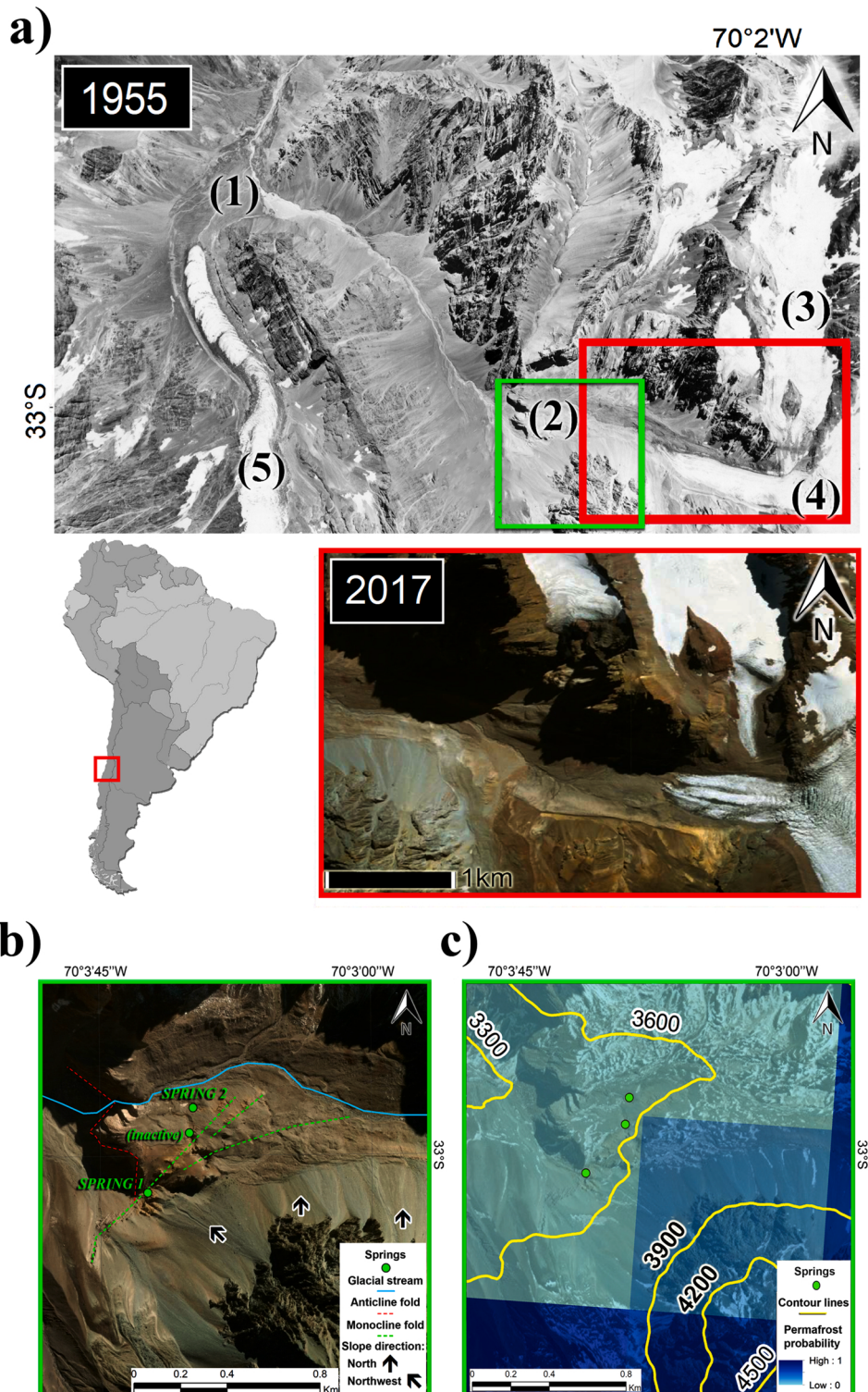


Fig. 1. Location of “Monos de Agua” catchment in the Central Andes. In (a), an Hycon aerial image (1955) with local inserts in red and green squares (Landsat 8, 2017). In (a), (1) is an outwash plain at 2700 m a.s.l., (2) are ground surface thermal loggers at 3200–3600 m a.s.l., (3–5) are “Monos de Agua” (local name “León Negro”), “Alto del Plomo” and “Juncal Norte” glaciers. (b) is the green insert in (a), showing groundwater spring sampling locations. In (c), permafrost probability (Obu et al., 2019) is shown for the equivalent area of study and contour lines every 300 m.

(Boisier et al., 2018; Cordero et al., 2019) and expect further snowpack loss of up to 75–85% by the year 2100 (Bozkurt et al., 2018), as well as increasing glacier and permafrost retreat (Baraer et al., 2012). In mountainous permafrost regions like the Andes, climate feedbacks between land and the atmosphere (Obu, 2021) affect the magnitudes of groundwater recharge (Green et al., 2011; Kuchment et al., 2000), summertime discharge (Gascoin et al., 2011) and ultimately its contribution to streamflow (Evans et al., 2015).

In proglacial aquifers, groundwater is actively recharged by glacier meltwater and local precipitation (O'Dochartaigh et al., 2019) and buffers river baseflow during the dry season (Mackay et al., 2020). For coarse-sediment alpine aquifers, there is first a fast discharge recession after the recharge season (e.g., snowmelt) or rainfall events, followed by a slow recession that sustains discharge over a long period (Hayashi, 2020). For instance, post-freshet baseflow (groundwater) ranges between 32% and 52% at glacierized headwater catchments (Liu et al., 2004; Baraer et al., 2009; Rodriguez et al., 2014; Evans et al., 2015). Such mountainous areas are often dominated by sedimentary disturbance regimes indirectly conditioned by glacial influence (Slaymaker, 2009), implying that coarse-grained features may buffer snowmelt transmission (Kurylyk and Hayashi, 2017) and constitute conduits for groundwater (Somers and McKenzie, 2020). Consequently, groundwater recharge via coarse slope deposits and moraines can be ultimately delayed by finer sediments and discharge to valley springs (Glas et al., 2018).

In mountainous periglacial environments, the thawing of ground ice acting as a thermal aquitard affects ground hydraulic transmissivity and may deliver distinctive signatures in water content which could differ from that of precipitation and seasonal surface water sources. Thus, permafrost degradation (e.g., due to climate change) influences surface and subsurface hydrologic conditions (Kurylyk et al., 2014), water quality (Szopińska et al., 2016; Toohey et al., 2016) and further determine the hydrologic behavior and water contribution of melting ground ice (Arenson et al., 2022).

Under the RCP8.5 scenario, groundwater recharge at 33° S is mainly due to snowmelt, while at 27° S, it is expected to be more driven by evapotranspiration (Wu et al., 2020). Hence, snowmelt partitioning between surface runoff and groundwater flow (soil ice-saturation inversely proportional to effective permeability) could increase storage in a thickening active-layer (Evans and Ge, 2017). Additionally, under slower snowmelt rates (due to season contraction), hydrological connectivity may not exceed necessary wetness thresholds (Musselman et al., 2017), leading to reduced streamflow, increasing dry season water stresses (Evans et al., 2018) that could generate less streamflow as infiltration fills previously depleted parts of the system (Alvarez-Garreton et al., 2021).

Hence, assessing changes in groundwater recharge sources and rates is critical for understanding the vulnerability of the cryolithic water environment to a changing climate upon permafrost degradation (Hiyama et al., 2013). For example, in permafrost degrading areas, baseflow would increase due to higher transmissivity, recharge, and storage, while in warmer areas under permafrost conditions, baseflow increases due to more increased regional (horizontal and vertical) connectivity (rerouting) (Evans et al., 2020).

This study focuses on the in-situ characterization of a mountain cryosphere system in a warming, semi-arid region under current ice-front retreat and an ongoing precipitation decline. We investigate whether the seasonal signature from groundwater springs can be associated with thawing sources and multiannual storage at proglacial aquifers, delivering insights on hydrological connections therein. We assessed a proglacial aquifer under permafrost conditions within the Aconcagua catchment in Central Chile at 33°S, expecting isotopic signals to drift from late spring to early autumn as snowmelt influence fades out.

The novelty and representativity of the current work are bound to deliver insight into hydrological connections present in mountain (paraglacial) environments where non-glacial processes are directly conditioned by glaciation (Slaymaker, 2009) and under permafrost conditions. Such settings represent current-day landscapes at the Aconcagua basin and other glacierized catchments in permafrost regions like the Himalayas, the Alps, and even Svalbard, where proglacial aquifer buffering processes are still difficult to assess.

2. Methods

We propose a methodological strategy using different proxies to understand the timeframes and connections involved in groundwater storage. The strategy takes advantage of the complementarity of hydrochemical and biological proxies to establish hydrological interpretations. We utilized anthropogenic gases, water isotope enrichment (deuterium and ^{18}O), and decay (tritium), as they have been used for decades to analyze snow runoff in mountain (Dincer et al., 1970) and lowland permafrost environments (Burn and Michel, 1988). To further differentiate groundwater sources, we looked at microbial composition (Bochet et al., 2020; Ramírez et al., 2020) found in alpine environments (Frey et al., 2016), presenting unique niche-dependent sequences of Proteobacteria (Sajjad et al., 2021). Consequently, we considered that water samples from point locations (streams and springs) could be differentiated by biological (representative of niche conditions) and different isotopic/gas signatures to the current atmospheric background (snow) between seasons.

2.1. Study site

Between 32°40'–32°56'S, the Aconcagua river runs westwards starting from headwater catchments between 3000 and 5100 m a.s.l. In 2018 and 2019, the Chilean Public Works Ministry passed decrees to officially declare the Aconcagua basin a water-scarce region, as it faces a sustained regional glacier shrinkage of over 30% of its total surface (Fig. 1) between 1955 and 2016 (Bodin et al., 2010; Monnier and Kinnard, 2017). Therein, the “Juncal River” sub-basin has an area of 342 km², and is located 75 km northeast of Santiago de Chile, with a mean air temperature between 1979 and 2016 of –3.1 °C at 3600 m a.s.l. (Boisier et al., 2018) and median annual precipitation of 581 mm (Alvarez-Garreton et al., 2018). The catchment's dominant input (>50% of peak) during melt season (mid-October until April) is glacial melt rather than snowmelt, the latter being the dominant input only during spring (mid-October to mid-November) (Ohlanders et al., 2013). More recently, streamflow contribution for the Aconcagua upper sub-basin ranges between 18% and 34% of glacial melt input and 20% on average for groundwater and periglacial sources (Crespo et al., 2020a, 2020b).

Fig. 1 shows a 1955 aerial photograph of the “Juncal River” sub-basin with the specific headwater catchment of study Monos de Agua (MA) in the red frame insert. The area lies within “Juncal Andean Park,” a private biodiversity conservation project that regenerated the valley after cattle-raising and mining activities. This catchment has had a consistent ice-retreat above 3600 m a.s.l. and sediment resettling as in most paraglacial environments (Ruiz Pereira and Veetil, 2019).

Rodriguez et al. (2016) described the eastern (highest) part of the “Juncal River” sub-basin as having mainly limestone and calcareous sandstone coexisting with igneous formations. Gypsum can be found in the northeast of the sub-basin, still, the local lithology is mostly volcano-sedimentary strata in the central and western parts (dacitic, pyroclastic, and basaltic rocks). Quaternary sequences consist of alluvial, colluvial, and in a lesser proportion fluvio-glacial deposits (Bown et al., 2008). Lithological details are in Additional Fig. 1.

In general, favorable conditions for permafrost occurrence within the Aconcagua basin are above 4000–4200 m (Gruber, 2012; Saito et al., 2016) with a fringe level between 3600–3900 m a.s.l. (Bartsch et al., 2016). Other mapping products locate mid and high-probability for permafrost above 3400 m and 4200 m a.s.l. (Obu et al., 2019; Ruiz Pereira et al., 2021; Tapia Baldis and Trombotto Liaudat, 2019).

Groundwater spring sampling was performed at two specific locations. For the fieldwork period between 2019 and 2020, out of three groundwater springs at 3600 m a.s.l. (Fig. 1b) one was always inactive when visited during fieldwork. Spring-1 was always found active during our fieldwork between November-April (from springtime to summer), and Spring-2 was active only from February-April (summer). Fieldwork during austral Autumn/Winter after April was impossible due to Park permits and the closing of roads due to snow.

2.2. System conceptualization

We estimated the time the water travels within the subsurface as a proxy for storage time, flow pathway heterogeneity, and hydrological source within the catchment (McDonnell et al., 2010). We investigated whether groundwater spring samples contained a biological signature (16S rRNA metabarcoding) associated with thawing sources (a cryotic microenvironment).

The system assumption considered a steady-state influx of multiyear, multi-entry points for surface infiltrations from an upper reservoir (roughly analogous to the vadose zone) with either a surface runoff outflux (stream) or seasonal quickflow from a lower reservoir (saturated zone) to groundwater springs (Fig. 2). The recharge considers infiltration of glacial/snow water (above 3600 m a.s.l.) and discharge from snowmelt, glacial melt, or interstitial water from permafrost thaw through groundwater springs at ~3600 m a.s.l. Groundwater spring streamflow measurements between 2019 and 2020 included cross-sections at the closest flat surface from the ground outflow by float method.

We account for soil responsiveness (Hrachowitz et al., 2009) from either aquitards (transmissivity lag) or aquiclude (impervious barrier) as discontinuous layers supporting perched groundwater (Hayashi, 2020) coupled with multi-entry proglacial (ice-cored) moraines (Langston et al., 2011). We consider that sources feeding groundwater springs could contain a thawing fraction (θ) from multiannual storage and are significantly distinct from surface water isotope and genetic makeup composition.

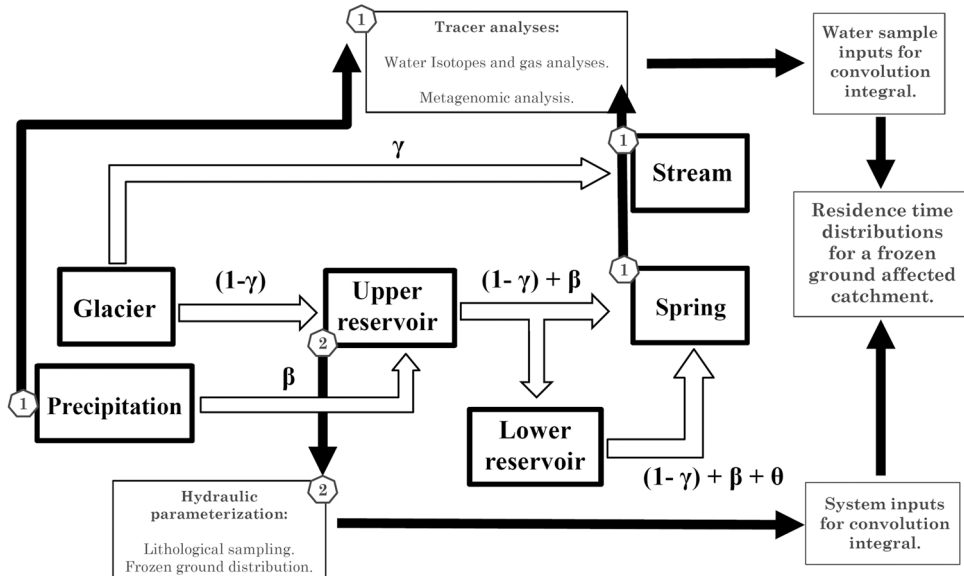


Fig. 2. Conceptual hydrological flow and transport model for the study catchment. The flowchart shows the assumed hydrological flow paths within the catchment. Precipitation is β ; the surface signal is γ with a complementary previously-stored fractional $(1-\gamma)$, and the multiannual subsurface signal is θ . Hollow arrows represent conceptual processes and filled arrows represent methodological processes in this study. The (1) polygons represent samples for water isotope analyses and (2) the hydraulic parameterization.

By using a linear steady-state mixing approach, we differentiated isotope background concentrations as snow precipitation signals (β) from surface (γ) fractions flowing through reservoirs in the catchment (Fig. 2). We followed a simple conceptualization by (Rose, 2007), where fractions (γ) of the total volume of the groundwater reservoir are released to base flow while the remaining fractions (1- γ) thoroughly mix with new inputs from the upper precipitation mixing reservoir.

Water isotope analysis requires controlling atmospheric precipitation background levels for the Andes (Houston, 2007) and considering that different transit time estimations are produced from equivalent ^3H concentrations due to radioactive decay (Stewart et al., 2010). Since the catchment is under mountain permafrost conditions (heterogeneous distribution) and there might be mean transit times of less than a year (Cochand et al., 2020), we associated an expression integrating (isotope) tracer values and the range of system response (flow regime) by combining hydraulic properties, tracer inputs, and outputs through a “lumped parameter” approach (Maloszewski and Zuber, 1996; Stewart et al., 2017).

2.3. Transit times

2.3.1. Hydraulic transit time estimation

The interpretation of a lower reservoir connected to groundwater springs required exploring flow model assumptions (Maloszewski and Zuber, 1982) under limited steady-state interpretation for confinement and unaltered traveling tracer concentrations (Leray et al., 2012). For example, turnover time (t_d) (McGuire and McDonnell, 2006) corresponds to a time magnitude (hydraulic residence time) estimated by assuming different spatial combinations of the system's state and integrating them with hydraulic properties determined from field samples:

$$t_d = n_e \frac{(\Delta l)^2}{k \Delta h} \quad (1)$$

n_e —effective porosity.

k —mean hydraulic conductivity.

Δl —distance from recharge to discharge.

Δh —height difference of the hydraulic head.

In terms of aquifer geometry, flow path length and height variation reflect the hydraulic driving forces of catchment-scale transport, e.g., Darcy's law (McGuire et al., 2005) and soil-type constraints (Rodgers et al., 2005). For example, sedimentary aquifers can take a wide range of hydraulic conductivity k values (1×10^{-5} to 1×10^{-2} m/s) (Sakata and Ikeda, 2013) as unconsolidated deposits (gravel, sands) can present effective porosity n_e ranging between 0.25 and 0.5 (Yu et al., 2015).

Therefore, hydraulic coefficients (Additional Table 1 and 2) considered lithological samples and hydraulic property values from literature (Domenico and Schwartz, 1998; Heath, 2004; Morris and Johnson, 1967). Additionally, considering paraglacial conditions (current sedimentary reworking due to ice-retreat), quaternary deposits (Additional Figs. 1 and 2) are assumed to have an approximate alluvium thickness between 1 and 11 m, with a median of seven meters (Mashburn et al., 2003).

The hydraulic conductivities and porosities in Eq. 1 considered values starting from semipervious to impervious sedimentary rock ($k = 10^{-6}$ to 10^{-5} m/s) (Bear, 1972), as well as the possible ranges for hydraulic head (Δh between 90 and 900 m) based on local topography and path length (Δl between 1.5 and 3.0 km). We considered for each parameter (hydraulic head, length, porosity, and conductivity) (Additional Table 1 and 2 and Additional Figs. 1 and 2) a hundred linearly spaced values, which resulted in a solution space with over 10^8 data points.

2.3.2. Water transit time analysis

Catchments receive tracer inputs (^{18}O , ^2H , ^3H , CFCs) and transport them through diverse flow paths, resulting in a distribution of transit times at sampling zones. The differentiation of hydrological fractions by hydrochemical analysis obeys two main criteria:

- (i) Origin within the hydrological cycle (snow, glacier, frozen ground).
- (ii) Reservoir location.

Limitations of using water stable isotopes for groundwater dating include that they are indicative of turnover-times only under five years (McGuire et al., 2005; Stewart et al., 2010) as detectable variation in ^{18}O is smaller than the measurement error (Stewart et al., 2021).

As an unstable hydrogen isotope, tritium has the advantage of being subjected to radioactive decay, a temporal difference easily calculated using regional calibration curves, especially in the Southern Hemisphere (Cauquoin et al., 2015), where the anthropogenic bomb peak did not exert such ambiguity as in Canada, Russia and China (Gibson et al., 2016; Makarov, 2016; Yi et al., 2018). Additionally, its short half-life of 12.3 years makes it appropriate for young and very young groundwater (Newman et al., 2010).

This study measured stable and unstable water isotope concentrations from snow composite, surface glacial stream, and groundwater springs. The sampling occurred between 3550 and 3590 m a.s.l. and between September-November 2018 (Austral Spring) and April 2020 (Austral winter).

Water samples were analyzed from specific locations:

- (a) Snow composite: background signal.
- (b) Glacial stream: surface water mix with multiannual storage signal.
- (c) Groundwater spring: subsurface water mix with multiannual storage signal.

Water isotope concentrations can be the input for calibrating the transit time distribution by fitting to measured tracer (sampling) output concentration (Maloszewski and Zuber, 1996). We chose to parametrize all inputs and outputs using a “lumped parameter” approach, which estimates a system’s dynamic (specifically, piston to exponential system response ratio) and describes integrated tracer transport through a catchment by discretizing physical constraints.

The lumped parameter may be explained by the following convolution integral (Dinçer et al., 1970);

$$C_{out} = \int_0^{\infty} C_{in}(t-\tau) e^{\lambda\tau} g(\tau) d\tau \quad (2)$$

This expression has $C_{out}(\tau)$, $C_{in}(\tau)$ system output and input (recharge) concentrations, t as calendar time, τ the transit time in system, λ the radioactive ${}^3\text{H}$ decay constant and $g(\tau)$ the system response function from assumed model.

We assumed a proglacial aquifer system consisting of quaternary coarse sedimentary areas with internal thickness-dependent structures affecting groundwater flow. We looked for the lowest number of fitting parameters for the number of sampling sites (Maloszewski and Zuber, 1993) and evaluated the system’s flow model and response type values, $g(\tau)$, as shown in Eqs. 3 and 4:

$$g(\tau) = 0 \quad (3)$$

$$\text{for } \tau < \tau_m(1 - \frac{1}{n})$$

$$g(\tau) = \left(\frac{n}{\tau_m} \right)^{\left(\frac{-\tau}{\tau_m} + n - 1 \right)} \quad (4)$$

$$\text{for } \tau \geq \tau_m(1 - \frac{1}{n})$$

τ_m represents the Mean Transit Time (MTT), τ the entry time of tracer (Chattarjee et al., 2019) and n as the ratio of the piston to exponential flow (EPM) aquifer area ranging from (+1) to (+6). The EPM is the ratio of the piston to exponential flow aquifer area, and the piston flow component can represent young groundwater that traveled vertically within the recharge zone.

The mean transit time (residence time) is integrated throughout different flow regime assumptions in Eq. 2.

Values considered the lowest measured tritium uncertainty and a more comprehensive range considering two half-lives from the snow background level. The value range for as τ_m inputs considered up to 60 years following other methodologies using tritium (Hiyama et al., 2013; Kralik, 2015).

The complex distribution of catchment flow paths is represented by a distribution of transit times describing tracer transport through the catchment. The assumption is that an annual hydrological flush promotes seasonal and multiannual isotopic stability for a steady-state isotope balance model (Gibson et al., 2015) and no concentration gradient throughout the catchment, or at least from the lower reservoir to the sampling output. For example, average groundwater residence time estimates between 14 and 18 years have been associated with aquifers accounting for 10–20 m thick regolith, 20–30% regolith/bedrock porosity, and hydraulic conductivity between 1.0e-08–1.2e-05 m/s (Rose, 2007).

In the present case, we estimated time-related distributions from water isotope measurements (${}^2\text{H}$ and ${}^{18}\text{O}$, and ${}^3\text{H}$). Water stable isotopes were measured in the Stable Isotope Laboratory of the Andres Bello University (Viña del Mar, Chile). Tritium measurements were performed at GNS Science (New Zealand, 2019) and Isotoptech Zrt. (Hungary, 2020–2021) by electrolytic enrichment and later measured by scintillation detectors with a resolution of 0.02 TU.

Surface snow samples as background tritium values were normalized (Eq. 5) to their field sampling time (Yi et al., 2018) as is a standard procedure (Houston, 2007). In the Southern Hemisphere, the tritium peak due to atomic energy testing is neglected and assumed stabilized (Cauquoin et al., 2015). Residence time distributions using tritium values considered a range using both the uncertainty (0.02 TU) and two half-lives from the snow background level (0.02–18 TU).

$$N_r = N_i * e^{-T/17.93} \quad (5)$$

N_i = Initial Tritium Concentration of given waterbody.

N_r = Residual Tritium concentration after time-defined radioactive decay.

2.4. Seasonal thaw

In addition to point source differentiation, seasonal differences are also expected. An isotopic separation between river water and precipitation ($\Delta 18\text{O}$) will depend on elevation and Mean Annual Air Temperature (MAAT) to account for stable isotope enrichment from thawing events.

$$\Delta^{18}\text{O} = \delta_{\text{PRECIPITATION}} - \delta_{\text{SOURCE}}$$

(6)

The estimation reflects runoff augmentation by water sources such as permafrost thaw or glacial melt with $\Delta^{18}\text{O} \geq 0$. For example, in Yukon (Canada), (Gibson et al., 2020) screened stable isotopes throughout areas under permafrost and found enrichment in streams from thawing grounds.

2.5. Open or closed groundwater system

Groundwater springs may constitute outputs from a closed system, for example, the thawing of interstitial ice or a rock glacier, but also a mixed recharge from snow, ground ice, and glacial water. Human emitted gas (CFC's and SF6's) concentrations aid the interpretation of surface/subsurface connection. CFC and SF6 concentrations in groundwater spring samples were measured at GNS Science in New Zealand by gas chromatography method with electron capture. Uncertainty for CFC and SF6 was 1.2% and 3%, respectively.

If the system is closed, the gas concentrations will be theoretically higher than current atmospheric levels. Still, if the system is partially open, levels will be equivalent to the current atmospheric ones.

2.6. Environmental genetic analyses

In this study, we utilized a biological proxy to understand the hydrological origin and connectivity of groundwater springs in paraglacial environments (at least two kilometers away from glacier termini). The diversity and composition of the prokaryotic community were analyzed from two spring sources where water was collected in April 2019. A hundred liters of water from each Spring-1 and Spring-2 (Fig. 1) were pumped through a 50 µm polyester net to exclude large organisms and particles and transported in darkness to the Microbial Ecology of Extreme systems laboratory (Pontificia Universidad Católica de Chile, Santiago, Chile). In the laboratory, samples were subjected to serial filtration using a peristaltic pump (6–600 rpm; pressure up to 2 bar) through 3 µm polycarbonate filters and 0.22 µm Sterivex filters (Millipore). Filters were maintained at –80 °C until nucleic acids extraction. DNA extraction used both filter fractions using a commercial DNeasy PowerSoil (Qiagen) kit.

DNA quantification was performed using a Qubit® 2.0 Fluorometer (Thermo Fisher Scientific, USA). Quality assessment utilized spectrophotometry (A260/A280 ratio) and integrity by standard agarose gel electrophoresis. Subsequently, PCR amplifications and mass sequencing of the 16S rRNA genes used primers 515 f and 926r to amplify the V4-V5 region (~376 bp) (Parada et al., 2016) (Illumina MiSeq platform; Argonne National Laboratory, Illinois, USA).

Raw sequences of the 16S rRNA gene were imported to the QIIME2 platform (v2019.7) (Bokulich et al., 2018; Bolyen et al., 2019; Caporaso et al., 2010) and demultiplexed (q2-demux plugin). Then, the paired-end sequences were trimmed and merged using DADA2 (Callahan et al., 2016) to obtain the Amplicon Sequencing Variants (ASVs).

ASVs taxonomy was assigned with the q2-feature-classifier (classify-consensus-vsearch) (Rognes et al., 2016) using the SILVA132 database (Quast et al., 2012). ASVs classified as “Mitochondria”, or “Chloroplast” were filtered out for the analysis of the Bacteria and Archaea community. Sequences from 3 and 0.2 µm fractions were mixed for each source (JS1 and JS2).

Finally, to remove singletons and rare taxa, ASVs were filtered by frequency (ASVs with >2 counts) and by taxonomy (Phyla with >2 ASVs) in the R package phyloseq (McMurdie and Holmes, 2013; Team, 2020). Alpha diversity analysis was performed on the clean reads with phyloseq and Vegan packages (Oksanen et al., 2019), considering observed diversity from Shannon and Simpson indexes (Wagner et al., 2018).

3. Results

3.1. Flow system characterization from water sample analyses

We considered that at least 15% of the “Monos de Agua” catchment area is currently under permafrost conditions (Fig. 1-c) predominantly above 4200 m a.s.l. (Ruiz Pereira et al., 2021), with negative mean annual ground surface temperatures below –2 °C. Between 3900 and 4200 m a.s.l., permafrost exists intermittently on shaded south-facing slopes.

The seasonal comparison between December and April 2019 shows similar deuterium levels for both sources in December but very different in April samples (Additional Table 3). The ^{18}O concentration also changed significantly, with differences between sources diverging from December to April. Additionally, the average $\Delta^{18}\text{O}$ between surface sources (springs and stream) and snow increased by 28% towards the end of the warm season of 2019 (Additional Table 7).

Comparing the 2019 and 2020 warm seasons, the isotopic signal (D and ^{18}O) for groundwater springs and glacial stream showed

Table 1

Water isotope analyses for groundwater springs and surface streams at 3600 m a.s.l. Measurements from late summer (April-May) 2019–2021.

Site ID	δD ‰ VSMOW ± 0.8	±	$\delta^{18}\text{O}$ ‰ VSMOW ± 0.1	±	d-excess	±	Tritium (TU)	±
Snow	-129.52	37.85	-17.04	4.89	6.81	1.31	6.39	2.66
Spring 1	-135.27	7.09	-18.25	0.77	10.76	1.42	2.12	0.56
Spring 2	-137.02	8.18	-18.47	0.89	10.71	1.28	2.63	0.15
Stream	-141.93	6.07	-19.18	0.62	11.49	1.69	2.08	0.77

distinct concentrations for hydrological sources (Table 1 & Additional Fig. 3a). The stable isotope levels measured for Spring 1 and the glacial stream showed an enriched signal.

The tritium values for the snow composite (September–November 2018 and April 2020) were 6.39 ± 2.66 TU, which we considered the background. The average tritium for groundwater springs (Spring 1 and 2) sampled in April 2019–2020 was 2.38 ± 0.44 TU, while the glacial stream was 2.13 ± 1.04 TU (Table 1 and Additional Fig. 3c). Between 2019 and 2021, the multiannual tritium signal for Spring 2 changed by 10%, while Spring 1 up to 60% (Additional Table 3).

The water isotope concentration ratios (Table 1 & Additional Table 3) showed that groundwater springs and stream samples are significantly lighter than the snow background in tritium but only showed a tendency in stable isotope levels. Even though results indicate Spring 2 as a more differentiated source in late austral summer (April), the overall difference between groundwater springs and the stream samples is not statistically conclusive.

3.2. Metagenomic analysis

The prokaryotic 16S rRNA gene sequence taxonomic composition evidenced the presence and abundance of psychrophiles (low temperature adapted) obtained from groundwater spring samples. The estimated diversity values for (50 nm - 0.2 μm size fraction) prokaryotic communities were similar between springs for ASVs and Shannon index. However, differences in the presence and relative abundance of some populations between springs (Fig. 3) are shown in Additional Table 5.

The taxonomic identity (Fig. 3a) showed the highest relative abundance for phylum Proteobacteria mainly represented by Beta-proteobacteriales, seconded by phyla Bacteroidetes, with Flavobacteriales dominating the phylum. Fig. 3b shows genera representing > 1% of prokaryotic (Bacteria and Archaea) communities per spring. Minor and rare genera in Fig. 3c show the 30 most abundant < 1%.

Venn plots show shared and unique taxa (represented by ASVs) for springs at phylum (Fig. 3d), genera > 1% (Fig. 3e), and genera < 1% or “uncultured taxa” (Fig. 3f) levels. At the phylum level, there were 522 shared ASVs, but only 66 ASVs assigned to the > 1% genera communities.

The most abundant and exclusive Spring-1 ASVs from > 1% genera were *Thalassospira* (2.9%), *Flavobacterium* (1.9%) and

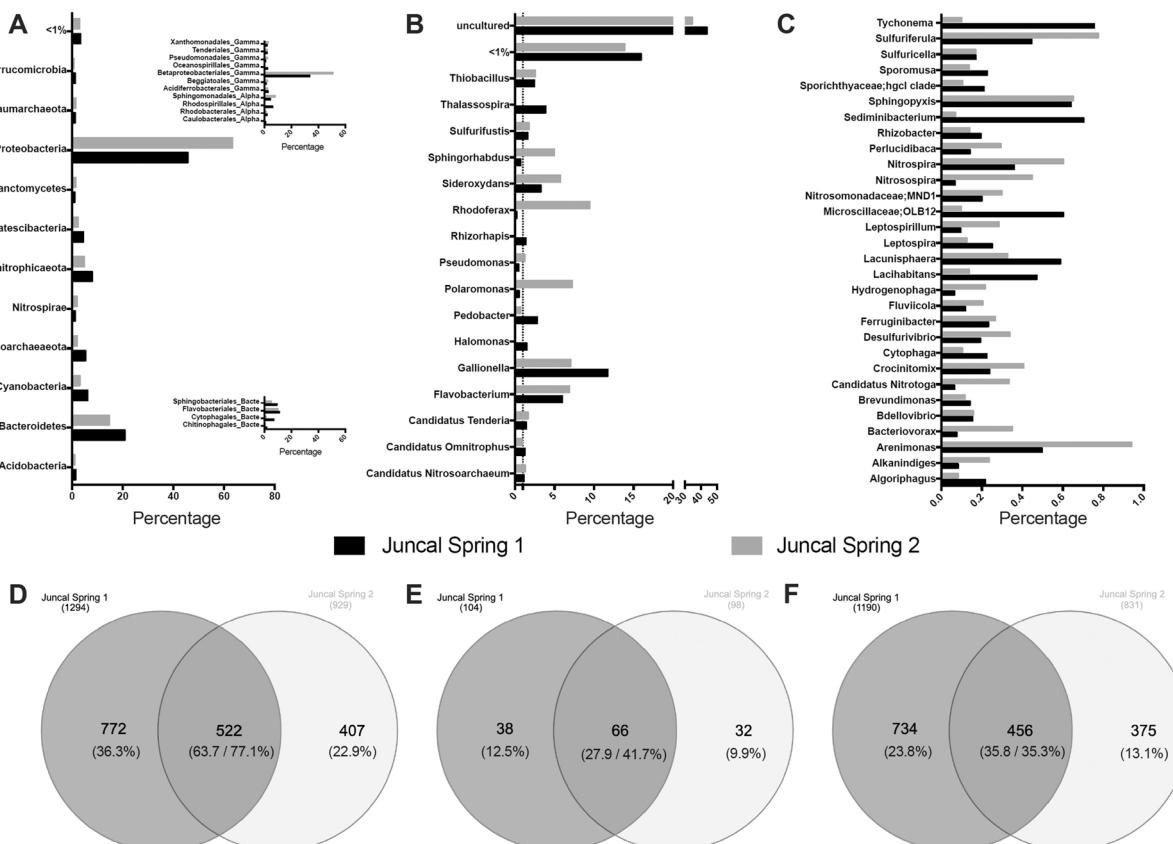


Fig. 3. Metagenomic analysis of 16S rRNA from groundwater springs. (A) shows relative abundance for phylum, (B) for prokaryotic > 1% genera and (C) for < 1% abundant genera. Venn diagrams show shared ASVs per phylum (D), (E) for > 1% abundant genera and (F) the < 1% abundant genera.

Halomonas (1.5%). For Spring-2 they were *Flavobacterium* (1.3%) and *Polaromonas* (2.6%). The most abundant ASVs in common for both springs were from genera representing > 1%, affiliated to *Gallionella*, *Sideroxydans*, *Thiobacillus*, *Flavobacterium*, *Rhodoferax*, and *Polaromonas*. Each of these ASVs was similarly abundant for both springs (representing 1–5% of the community), but the ASVs assigned to *Polaromonas* and *Rhodoferax* were substantially more abundant in Spring-2 (Fig. 3b). The high number of unique ASVs observed between springs denotes the differences in bacterial community composition.

Polaromonas is a known psychrophile. Some species of *Rhodoferax* could also be considered “psychrotolerant” and grow near 0 °C like *R. antarcticus*, recovered from glacial habitats (Madigan et al., 2000), or *R. ferrireducens* isolated from anaerobic subsurface aquifer sediments (Finneran et al., 2003). The other shared genera (*Thiobacillus*, *Gallionella*, *Sideroxydans*) are (chemolithotrophic) nitrifying Betaproteobacterales commonly associated with iron oxidation and found in dark and iced environments, likely as primary producers, fixing carbon and weathering minerals, thus explaining how a such microbial ecosystem can be sustained in ice (Touzes-Rodrigo et al., 2017).

Additionally, other nitrifiers and Fe redox bacterial genera were present within the “minor and rare” (<1%) group. Spring-1 differed by showing a higher relative abundance of Bacteroidetes (Flavobacterales and Sphingobacterales orders) and twice as many Cyanobacteria (Fig. 3a,b).

The dominant bacterial members of Spring-2 (*Polaromonas* and *Rhodoferax*), together with other taxa also shared with Spring-1, are associated with a biogeochemical role in C cycling as primary producers, mainly as nitrifiers in N cycling in this environment.

3.3. Transit time analysis

Isotope-derived transit time (${}^3\text{H}/{}^{18}\text{O/D}$) estimation (Additional Table 3) resulted in 4.77 ± 2.05 years. The “lumped parameter” approach had a system response ($G(t)$) with a n ratio (EPM) value (4.17 ± 1.17). The convolution outputs in Fig. 4 show a predominant peak around five years of mean transit time with only tritium outputs spanning longer than a decade, which is consistent with the ‘truncation’ hypothesis (Stewart et al., 2021).

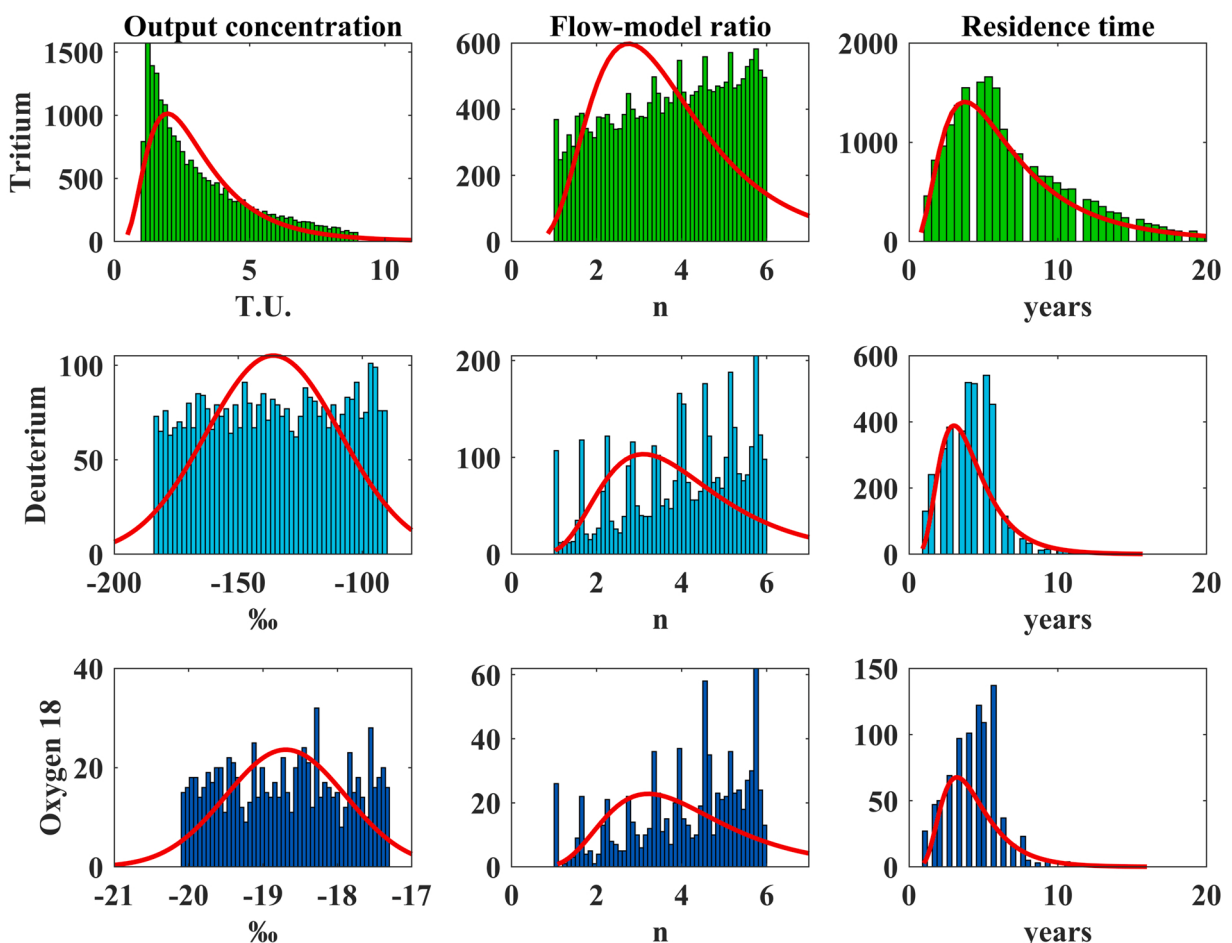


Fig. 4. Convolution integral with rows for tritium, deuterium, and ${}^{18}\text{O}$. The “Flow model” column shows the Exponential to Piston Flow ratio (n) and residence time shows all transit time outputs.

This range of transit time values does fall within the hydraulic turnover time estimation from Eq. 1 was 13.67 ± 20.09 years (Additional Fig. 4), especially with the longer tails of tritium outputs beyond a decade.

3.4. Interstitial water volume under cryogenic conditions

The volume associated with thawing outflowing at groundwater springs between 2019 and 2020 considered streamflow measurements, apparent transmissivity, and porosity data from field samples and literature (Additional Table 1 and 2). The streamflow was measured at $0.14 \pm 0.02 \text{ m}^3/\text{s}$ for Spring-1 and $0.14 \pm 0.01 \text{ m}^3/\text{s}$ for Spring-2.

The total possible volume of groundwater stored in the aquifer was calculated using a conservative estimate (Ó Dochartaigh et al., 2019) of average aquifer porosity (Additional Figs. 1 and 2) above 3600 m a.s.l and corresponded to 2.52 km^3 (Additional Fig. 2). Consequently, considering a mean spring streamflow of $0.141 \text{ m}^3/\text{s}$, the estimated annual volume per a minimal ninety-day thawing season is at least 0.004 km^3 assuming the average travel time of around four years with no additional recharge. Therefore, Spring 2 accounts for approximately 0.004 km^3 , associated with warm season thawing groundwater and representing less than a 0.2% of the total vadose volume.

4. Discussion

We estimated timescales for groundwater flow dampening at a proglacial foreland under permafrost conditions, implying recharge from glacial melt and snow infiltration later outflowing through groundwater springs. An inferred multiannual storage indicated glacier-permafrost connections evidenced through thawing signals during the late warm season using isotopic and biological analyses. The evidence supports our interpretation of a dampened downstream flow signal in proglacial aquifer areas, which could alter long-term hydrologic trends over heterogeneous landscapes (Chezik et al., 2017).

Spring-2 represented a thawing cryogenic source during the warm season. It is inactive during early austral summer from our observations, and ground surface temperature data at that location showed negative temperatures starting in May (Ruiz Pereira et al., 2021). Since Spring-2 had this “late warm-season activation”, we argue that the two groundwater springs should have different origins (different reservoir, Fig. 2) and that Spring-1 is more connected to the surface and less likely related to thawing sources than Spring-2.

The anthropogenic gas levels (CFCs, SF₆) from springs resulted in equivalent to atmospheric levels for both springs (Additional Table 4 & Additional Fig. 3b) and therefore cannot be used in the “lumped parameter” approach to estimate residence times. However, they partially confirm that the groundwater systems are connected to the surface under a seasonal dynamic.

Groundwater springs and stream samples show stable-isotope seasonality between early and late summer 2019. This can be explained by the loss of a snow-dominated signal from flow path convergence and a high proportion of young water (Leray et al., 2016). For late summer sampling between 2019 and 2021, average groundwater spring tritium content of $2.38 \pm 0.67 \text{ TU}$ could constitute a mixture of only glacial melt and snow, as the glacial stream has a content of $2.08 \pm 0.77 \text{ TU}$ and snow is higher than both. Nevertheless, since stable isotopes in groundwater springs are lighter than in the glacial stream, a strictly seasonal (non-interannual storage) glacial origin for groundwater springs is not supported by linear mixing. Therefore, an additional mixing input from thawing is implied, assumed to have a different storage time and/or hydrological origin.

If groundwater springs are glacial melt flowing underground and emerging in late summer, the tritium content should not differ from that of the glacial stream. However, if spring samples are only mixtures of snow and interstitial ice (thawing input), ice tritium content should be higher than the current background (Cauquoin et al., 2015; Houston, 2007; László et al., 2020) to match the stable isotope levels. In fact, tritium from Spring 2 is less depleted than the surface runoff signal (stream) (Table 1) and has a “lighter” D/¹⁸O content, implying an intermediate mixture. Moreover, stable water isotopes from the glacial stream are equal to or more enriched than snow precipitation ($\Delta^{18}\text{O} > 0$), which is consistent with water balance processes modifying initial precipitation isotope signatures (Gibson et al., 2020) and a signal of thawing environments (Wan et al., 2019; Yi et al., 2018). Therefore, the average residence time implies that the largest outflux fraction belongs to young groundwater (Kazemi et al., 2006) with multiannual storage under permafrost conditions. Nevertheless, residence times beyond five decades could not be derived as tritium calibration curves are unavailable beyond such timescales for ‘modern groundwater’ interpretations.

The positive $\Delta^{18}\text{O}$ values represent a seasonal thawing signal consistent with (Crespo et al., 2017) and (Crespo et al., 2020a, 2020b) in the same region (Additional Table 7). The δ-excess values (Dansgaard, 1964; Zech et al., 2013) shown in Table 1 increased during warmer summer, with both Spring-1 and 2 having virtually the same excess. These values are in concert with the increase in warm season mentioned by Froehlich et al. (2008) and Crespo et al. (2017), which also showed low δ-excess snow samples consistent with more evaporative conditions.

Metagenomic analyses of 16S rRNA allowed identification and comparison between springs, showing differences in the presence and abundance of both major (>1% of the total community) and minor/rare (<1%) taxa between springs, reinforcing the idea that Spring-2 may represent a seasonal thawing niche. The finding is consistent with analyses from Alaska, where *Rhodoferax ferrireducens* was abundant in permafrost (Hultman et al., 2015), the Swiss Alps, with Betaproteobacteria such as *Polaromonas* and *Rhodoferax* associated with the permafrost layer (Frey et al., 2016) and also 15,000 year old ice cores from the Tibetan Plateau (Zhong et al., 2021). Furthermore, in permafrost areas of the Dry Andes (27° S), Aszalós et al. (2016) and Aszalós et al. (2020), found *Rhodoferax ferrireducens* (6500 m a.s.l), *Flavobacterium* and *Polaromonas* (5900 m a.s.l.) in cold water samples from shallow lakes.

These results imply that sequences from groundwater spring samples potentially come from a putative subsurface habitat with freezing-thawing conditions and that groundwater spring connectivity should have a seasonal evolution, as suggested by tritium and microbial metagenomic identity.

Transit times derived from hydraulic and isotopic analyses under a year (Cochand et al., 2020) are assumed from the “upper reservoir” fractions, while longer tails (Fig. 4) would be associated with a “lower reservoir”. Spring-2 can ultimately be recognized as coming from thawing frozen grounds in late-summer but representing a sub-decadal recharge, meaning it is a mix of both snow and glacial water with multiannual storage. This interpretation resembles spring water analyses in Siberia, showing bipartite composition containing older precipitation recharge and water partly sourced from thawing permafrost (Hiyama et al., 2013) but not a true permafrost thawing origin modulating water input signals into discharge signals (Arenson et al., 2022).

In the future, with earlier and lesser snowmelt (Musselman et al., 2017) and increased frozen ground degradation (Evans and Ge, 2017), the hydrological connectivity could be disrupted by not exceeding necessary wetness thresholds and compromising groundwater storage dynamic (Green et al., 2011). For example, in proglacial areas under permafrost conditions, the underestimation of river flow can be explained by groundwater temporarily buffering glacier melt (Somers et al., 2019) but also by the neglect of groundwater flow from ephemeral streams draining from hillslopes as well as subsurface seepage from surrounding moraine systems (Ó Dochartaigh et al., 2019). These processes will affect the interannual variability of glacier meltwater (Saberi et al., 2019) and future river flow estimations (Chezik et al., 2017), hence the need for timeframes of interannual storage in glacial forelands.

Furthermore, as connectivity changes, microbial habitats will also be affected. For example, an increasing temperature in frozen soils could increase the relative abundance of Proteobacteria and Bacteroidetes taxa (Luláková et al., 2019), and condition microbial communities (Ballhausen et al., 2020). Therefore, the current genetic taxonomic configuration of such communities then constitutes a proxy for subsurface variations as an indirect way of assessing the temporal variability of groundwater environments. Future bioinformatics analyses comparing ground ice microbial metagenomics should deliver more concrete ideas on what to expect from samples belonging to seasonal thawing.

The limitations of the presented methodological strategy require a higher temporal sampling resolution necessary to surpass uncertainties bound to interannual variations of precipitation and ground surface temperatures conditioning infiltration. Additionally, the mixing possibilities for a proglacial aquifer system imply that the retrieved data does not allow discerning between the glacial stream and interstitial ice in terms of their spatiotemporal origin. Glacier and ground ice background isotopic signatures are also an ideal reference for refining results such as those obtained by the present work. Nevertheless, to avoid the complexity and costs implied in high mountain prospection, one complementary option is particle tracking simulations to obtain residence time distribution representing the different possibilities of groundwater storage and flow within a proglacial aquifer. This may allow the statistical discretization of groundwater sources, especially the subsurface structure, which may include transitional layers amongst frozen grounds, also subject to inter-annual variability of surface temperatures and precipitation. Additionally, the development of environmental tritium derived from atmospheric circulation models and ice-cores could be complementary for understanding the variation of tritium as background beyond the scope of modern groundwater.

5. Conclusions

Our three-year analysis determined multiannual groundwater storage at a proglacial aquifer under permafrost conditions at 33° S in the Andes mountains. During summer 2019–2021, groundwater springs at proglacial areas presented stable isotope enrichment, depleted tritium content, and indications of thawing. One spring was activated during the late warm season only, and its microbial metagenomic analysis by 16S metabarcoding, showed taxa common to mountain glaciers and lowland permafrost environments (*Polaromonas* and *Rhodofex*), indicating a thawing environment as a source sustaining such psychrophile diversity. The hydraulic and isotope-derived transit time equations delivered distributions suggesting multiannual groundwater storage under a decade. Results indicate that proglacial aquifer groundwater recharges from glacial meltwater, precipitation, and frozen-ground sources such as interstitial ice. The interpretation is a sub-decadal dampening timescale of proglacial groundwater storage, which should be considered in hydrological budgets that include paraglacial mountain areas under current ice-retreat.

The integrative methodological strategy was adequate to unveil hydrological timeframes for hydric potential in rapidly evolving proglacial settings within water-scarce regions. Using genetic proxies improves the understanding and interpretation of water samples by indirectly ascribing a likely origin, such as a seasonal thawing source, and represents a valuable tool to assess remote mountainous areas for preliminary interpretations of their hydrological connections. For example, if future snowmelt partitioning extends through newly available subsurface flow paths, and increases hydrological connectivity, then unique microbial habitats would also undergo selective pressure and may constitute a proxy for the subsurface biochemical evolution of frozen proglacial aquifers.

Much work is still required to thoroughly assess complex mountain systems with interconnected cryosphere elements, as they often evolve in a nonlinear fashion through different timescales. Hence, the present methodological approach would greatly benefit from higher sampling resolution and further bioinformatic comparison with genetic results from ground and glacial ice samples but also integrating groundwater particle tracking simulations to establish water isotope variation and transit time ranges.

Declaration of Competing Interest

The authors declare that they have no known competing financial interests or personal relationships that could have appeared to influence the work reported in this paper.

Acknowledgements

We kindly acknowledge our colleagues Sergio Guajardo, Pablo Vergara, and Marianne Buscaglia for their assistance with sample

collection. We thank Tomas Dinges and the Parque Andino Juncal, DGA-MOP-Chile, Einer Sepúlveda, Hans Fernández and Rodrigo Soteres. This work was financially supported by Agencia Nacional de Investigación y Desarrollo de Chile (ANID) FONDECYT 1191223, FONDAP 1511009, and the VRI-UC ‘Interdisciplina’ Project II190086. The authors acknowledge the two anonymous reviewers and editors for their fruitful reviews, which significantly improved the manuscript.

Appendix A. Supporting information

Supplementary data associated with this article can be found in the online version at doi:[10.1016/j.ejrh.2022.101311](https://doi.org/10.1016/j.ejrh.2022.101311).

References

- Alvarez-Garreton, C., Mendoza, P.A., Boisier, J.P., Addor, N., Galleguillos, M., Zambrano-Bigiarini, M., Lara, A., Cortes, G., Garreaud, R., McPhee, J., 2018. The CAMELS-CL dataset: catchment attributes and meteorology for large sample studies-Chile dataset. *Hydrol. Earth Syst. Sci.* 22 (11), 5817–5846.
- Arenson, L.U., Harrington, J.S., Koenig, C.E.M., Wainstein, P.A., 2022. Mountain permafrost hydrology—a practical review following studies from the andes. *Geosciences* 12 (2), 48.
- Aszalós, J.M., Krett, G., Anda, D., Márialigeti, K., Nagy, B., Borsodi, A.K., 2016. Diversity of extremophilic bacteria in the sediment of high-altitude lakes located in the mountain desert of Ojos del Salado volcano, Dry-Andes. *Extremophiles* 20 (5), 603–620.
- Aszalós, J.M., Szabó, Á., Megyes, M., Anda, D., Nagy, B., Borsodi, A.K., 2020. Bacterial diversity of a high-altitude permafrost thaw pond located on Ojos del Salado (Dry Andes, Altiplano-Atacama Region). *Astrobiology* 20 (6), 754–765.
- Ballhausen, M.-B., Hewitt, R., Rillig, M.C., 2020. Mimicking climate warming effects on Alaskan soil microbial communities via gradual temperature increase. *Sci. Rep.* 10 (1), 1–10.
- Baraer, M., McKenzie, J.M., Mark, B.G., Bury, J., Knox, S., 2009. Characterizing contributions of glacier melt and groundwater during the dry season in a poorly gauged catchment of the Cordillera Blanca (Peru). *Adv. Geosci.* 22, 41–49.
- Baraer, M., Mark, B.G., McKenzie, J.M., Condom, T., Bury, J., Huh, K.-I., Portocarrero, C., Gómez, J., Rathay, S., 2012. Glacier recession and water resources in Peru’s Cordillera Blanca. *J. Glaciol.* 58 (207), 134–150.
- Barnett, T.P., Adam, J.C., Lettenmaier, D.P., 2005. Potential impacts of a warming climate on water availability in snow-dominated regions. *Nature* 438 (7066), 303–309.
- Bear, J., 1972. Dynamics of Fluids in Porous Media. Dover Publications.
- Bochet, O., Bethencourt, L., Dufresne, A., Farasin, J., Pédrot, M., Labasque, T., Chatton, E., Lavenant, N., Petton, C., Abbott, B.W., 2020. Iron-oxidizer hotspots formed by intermittent oxic-anoxic fluid mixing in fractured rocks. *Nat. Geosci.* 13 (2), 149–155.
- Bodin, X., Rojas, F., Brenning, A., 2010. Status and evolution of the cryosphere in the Andes of Santiago (Chile, 33.5 S.). *Geomorphology* 118 (3–4), 453–464.
- Boisier, J.P., Alvarez-Garreton, C., Cordero, R.R., Damiani, A., Gallardo, L., Garreaud, R.D., Lambert, F., Ramallo, C., Rojas, M., Rondanelli, R., 2018. Anthropogenic drying in central-southern Chile evidenced by long-term observations and climate model simulations. *Elem. Sci. Anth* 6 (1).
- Bokulich, N.A., Kaehler, B.D., Rideout, J.R., Dillon, M., Bolyen, E., Knight, R., Huttley, G.A., Caporaso, J.G., 2018. Optimizing taxonomic classification of marker-gene amplicon sequences with QIIME 2’s q2-feature-classifier plugin. *Microbiome* 6 (1), 1–17.
- Bolyen, E., Rideout, J.R., Dillon, M.R., Bokulich, N.A., Abnet, C.C., Al-Ghalith, G.A., Alexander, H., Alm, E.J., Arumugam, M., Asnicar, F., 2019. Reproducible, interactive, scalable and extensible microbiome data science using QIIME 2. *Nat. Biotechnol.* 37 (8), 852–857.
- Bown, F., Rivera, A., Acuña, C., 2008. Recent glacier variations at the Aconcagua basin, central Chilean Andes. *Ann. Glaciol.* <https://doi.org/10.3189/172756408784700572>.
- Bozkurt, D., Rojas, M., Boisier, J.P., Valdivieso, J., 2018. Projected hydroclimate changes over Andean basins in central Chile from downscaled CMIP5 models under the low and high emission scenarios. *Clim. Change* 150 (3–4), 131–147. <https://doi.org/10.1007/s10584-018-2246-7>.
- Burn, C.R., Michel, F.A., 1988. Evidence for recent temperature-induced water migration into permafrost from the tritium content of ground ice near Mayo, Yukon Territory, Canada. *Can. J. Earth Sci.* 25 (6), 909–915. <https://doi.org/10.1139/e88-087>.
- Callahan, B.J., McMurdie, P.J., Rosen, M.J., Han, A.W., Johnson, A.J.A., Holmes, S.P., 2016. DADA2: High-resolution sample inference from Illumina amplicon data. *Nat. Methods* 13 (7), 581–583. <https://doi.org/10.1038/nmeth.3869>.
- Caporaso, J.G., Kuczynski, J., Stombaugh, J., Bittinger, K., Bushman, F.D., Costello, E.K., Fierer, N., Pena, A.G., Goodrich, J.K., Gordon, J.I., 2010. QIIME allows analysis of high-throughput community sequencing data. *Nat. Methods* 7 (5), 335–336.
- Cauquoin, A., Jean-Baptiste, P., Risi, C., Fourré, E., Stenni, B., Landais, A., 2015. The global distribution of natural tritium in precipitation simulated with an Atmospheric General Circulation Model and comparison with observations. *Earth Planet. Sci. Lett.* <https://doi.org/10.1016/j.epsl.2015.06.043>.
- Chezilek, K.A., Anderson, S.C., Moore, J.W., 2017. River networks dampen long-term hydrological signals of climate change. *Geophys. Res. Lett.* 44 (14), 7256–7264.
- Cochand, M., Molson, J., Barth, J.A.C., van Geldern, R., Lemieux, J.M., Fortier, R., Therrien, R., 2020. Rapid groundwater recharge dynamics determined from hydrogeochemical and isotope data in a small permafrost watershed near Umiujaq (Nunavik, Canada). *Hydrogeol. J.* 28 (3) <https://doi.org/10.1007/s10040-020-02109-x>.
- Cordero, R.R., Asencio, V., Feron, S., Damiani, A., Llanillo, P.J., Sepulveda, E., Jorqueria, J., Carrasco, J., Casassa, G., 2019. Dry-season snow cover losses in the Andes (18°–40°S) driven by changes in large-scale climate modes. *Sci. Rep.* 9 (1), 16945. <https://doi.org/10.1038/s41598-019-53486-7>.
- Crespo, S., Aranibar, J., Gomez, L., Schwikowski, M., Brueetsch, S., Cara, L., Villalba, R., 2017. Ionic and stable isotope chemistry as indicators of water sources to the Upper Mendoza River basin, Central Andes of Argentina. *Hydrol. Sci. J.* 62 (4), 588–605.
- Crespo, S.A., Fernando, F., Cara, L., Klarian, S., Lavergne, C., 2020a. First snow, glacier and groundwater contribution quantification in the upper Mendoza River basin using stable water isotopes. *Isot. Environ. Health Stud.* 1–20. <https://doi.org/10.1080/10256016.2020.1797713>.
- Crespo, S.A., Lavergne, C., Fernando, F., Muñoz, A.A., Cara, L., Olfos-Vargas, S., 2020b. Where does the chilean aconcagua river come from? Use of natural tracers for water genesis characterization in glacial and periglacial environments. *Water Vol.* 12 (Issue 9). <https://doi.org/10.3390/w12092630>.
- Dansgaard, W., 1964. Stable isotopes in precipitation. *Tellus* 16 (4), 436–468.
- DeSA, U.N., 2013. World Population Prospects: The 2012 Revision. Population Division of the Department of Economic and Social Affairs of the United Nations Secretariat, New York, p. 18.
- Dincer, T., Payne, B.R., Florkowski, T., Martinec, J., Tongiorgi, E., 1970. Snowmelt runoff from measurements of tritium and oxygen-18. *Water Resour. Res.* 6 (1), 110–124. <https://doi.org/10.1029/WR006i001p00110>.
- Domenico, P.A., Schwartz, F.W., 1998. Physical and Chemical Hydrogeology, Vol. 506. Wiley, New York.
- Evans, S.G., Ge, S., 2017. Contrasting hydrogeologic responses to warming in permafrost and seasonally frozen ground hillslopes. *Geophys. Res. Lett.* 44 (4) <https://doi.org/10.1002/2016GL072009>.
- Evans, S.G., Ge, S., Liang, S., 2015. Analysis of groundwater flow in mountainous, headwater catchments with permafrost. *Water Resour. Res.* 51 (12), 9564–9576.
- Evans, S.G., Ge, S., Voss, C.I., Molotch, N.P., 2018. The role of frozen soil in groundwater discharge predictions for warming alpine watersheds. *Water Resour. Res.* 54 (3), 1599–1615.

- Evans, S.G., Yokeley, B., Stephens, C., Brewer, B., 2020. Potential mechanistic causes of increased baseflow across northern Eurasia catchments underlain by permafrost. *Hydrol. Process.* 34 (11), 2676–2690.
- Finneran, K.T., Johnsen, C.V., Lovley, D.R., 2003. Rhodoferax ferrireducens sp. nov., a psychrotolerant, facultatively anaerobic bacterium that oxidizes acetate with the reduction of Fe (III). *Int. J. Syst. Evolut. Microbiol.* 53 (3), 669–673.
- Frey, B., Rime, T., Phillips, M., Stierli, B., Hajdas, I., Widmer, F., Hartmann, M., 2016. Microbial diversity in European alpine permafrost and active layers. *FEMS Microbiol. Ecol.* 92 (3) <https://doi.org/10.1093/femsec/fiw018>.
- Gascoin, S., Kinnard, C., Ponce, R., Macdonell, S., Lhermitte, S., Rabatel, A., 2011. Glacier contribution to streamflow in two headwaters of the Huasco River, Dry Andes of Chile. *Cryosphere* 5, 1099–1113.
- Gibson, J.J., Birks, S.J., Yi, Y., Vitt, D.H., 2015. Runoff to boreal lakes linked to land cover, watershed morphology and permafrost thaw: a 9-year isotope mass balance assessment. *Hydrol. Process.* 29 (18), 3848–3861. <https://doi.org/10.1002/hyp.10502>.
- Gibson, J.J., Holmes, T., Stadnyk, T.A., Birks, S.J., Eby, P., Pietroniro, A., 2020. 18O and 2H in streamflow across Canada. *J. Hydrol.: Reg. Stud.* 32, 100754 <https://doi.org/10.1016/j.ejrh.2020.100754>.
- Glas, R., Lautz, L., McKenzie, J., Mark, B., Baraer, M., Chavez, D., Maharaj, L., 2018. A review of the current state of knowledge of proglacial hydrogeology in the Cordillera Blanca, Peru. *Wiley Interdiscip. Rev.: Water* 5 (5), e1299.
- Green, T.R., Taniguchi, M., Kooi, H., Gurdak, J.J., Allen, D.M., Hiscock, K.M., Treidel, H., Aureli, A., 2011. Beneath the surface of global change: impacts of climate change on groundwater. *J. Hydrol.* 405 (3–4), 532–560.
- Gruber, S., 2012. Derivation and analysis of a high-resolution estimate of global permafrost zonation. *Cryosphere*. <https://doi.org/10.5194/tc-6-221-2012>.
- Hayashi, M., 2020. Alpine hydrogeology: the critical role of groundwater in sourcing the headwaters of the world. *Groundwater* 58 (4), 498–510.
- Heath, R.C., 2004. Basic Ground-water Hydrology. US Geological Survey Reston, VA.
- Hiyama, T., Asai, K., Kolesnikov, A.B., Gagarin, L.A., Shepelev, V.V., 2013. Estimation of the residence time of permafrost groundwater in the middle of the Lena River basin, eastern Siberia. *Environ. Res. Lett.* 8 (3), 35040.
- Houston, J., 2007. Recharge to groundwater in the Turi Basin, northern Chile: an evaluation based on tritium and chloride mass balance techniques. *J. Hydrol.* 334 (3–4), 534–544.
- Hrachowitz, M., Soulsby, C., Tetzlaff, D., Dawson, J.J.C., Malcolm, I.A., 2009. Regionalization of transit time estimates in montane catchments by integrating landscape controls. In: *Water Resources Research*, 45. <https://doi.org/10.1029/2008WR007496>.
- Hultman, J., Waldrop, M.P., Mackelprang, R., David, M.M., McFarland, J., Blazewicz, S.J., Harden, J., Turetsky, M.R., McGuire, A.D., Shah, M.B., 2015. Multi-omics of permafrost, active layer and thermokarst bog soil microbiomes. *Nature* 521 (7551), 208–212.
- Kazemi, G.A., Lehr, J.H., Perrochet, P., 2006. Groundwater Age. John Wiley & Sons.
- Kralik, M., 2015. How to estimate mean residence times of groundwater. *Procedia Earth Planet. Sci.* 13, 301–306.
- Kuchment, L.S., Gelfan, A.N., Demidov, V.N., 2000. A distributed model of runoff generation in the permafrost regions. *J. Hydrol.* 240 (1–2), 1–22.
- Kurylyk, B.L., Hayashi, M., 2017. Inferring hydraulic properties of alpine aquifers from the propagation of diurnal snowmelt signals. *Water Resour. Res.* 53 (5), 4271–4285.
- Kurylyk, B.L., MacQuarrie, K.T.B., McKenzie, J.M., 2014. Climate change impacts on groundwater and soil temperatures in cold and temperate regions: implications, mathematical theory, and emerging simulation tools. *Earth-Sci. Rev.* 138, 313–334.
- Langston, G., Bentley, L.R., Hayashi, M., McClymont, A., Pidlisicky, A., 2011. Internal structure and hydrological functions of an alpine proglacial moraine. *Hydrol. Process.* <https://doi.org/10.1002/hyp.8144>.
- László, E., Palcsú, L., Leelössy, Á., 2020. Estimation of the solar-induced natural variability of the tritium concentration of precipitation in the Northern and Southern Hemisphere. *Atmos. Environ.* 233, 117605.
- Leray, S., De Dreuzy, J.-R., Bour, O., Labasque, T., Aquilina, L., 2012. Contribution of age data to the characterization of complex aquifers. *J. Hydrol.* 464, 54–68.
- Leray, S., Engdahl, N.B., Massoudieh, A., Bresciani, E., McCallum, J., 2016. Residence time distributions for hydrologic systems: mechanistic foundations and steady-state analytical solutions. *J. Hydrol.* <https://doi.org/10.1016/j.jhydrol.2016.01.068>.
- Liu, F., Williams, M.W., Caine, N., 2004. Source waters and flow paths in an alpine catchment, Colorado Front Range, United States. *Water Resour. Res.* 40 (9) <https://doi.org/10.1029/2004WR003076>.
- Luláková, P., Perez-Mon, C., Šantrúčková, H., Ruethi, J., Frey, B., 2019. High-alpine permafrost and active-layer soil microbiomes differ in their response to elevated temperatures. *Front. Microbiol.* Vol. 10, 668.
- Mackay, J.D., Barrand, N.E., Hannah, D.M., Krause, S., Jackson, C.R., Everest, J., MacDonald, A.M., Ó Dochartaigh, B.É., 2020. Proglacial groundwater storage dynamics under climate change and glacier retreat. *Hydrol. Process.* 34 (26), 5456–5473.
- Madigan, M.T., Jung, D.O., Woesz, C.R., Achenbach, L.A., 2000. Rhodoferax antarcticus sp. nov., a moderately psychrophilic purple nonsulfur bacterium isolated from an Antarctic microbial mat. *Arch. Microbiol.* 173 (4), 269–277.
- Maloszewski, P., Zuber, A., 1993. Principles and practice of calibration and validation of mathematical models for the interpretation of environmental tracer data in aquifers. *Adv. Water Resour.* 16 (3), 173–190.
- Maloszewski, P., & Zuber, A. (1996). Lumped parameter models for the interpretation of environmental tracer data.
- Maloszewski, P., Zuber, A., 1982. Determining the turnover time of groundwater systems with the aid of environmental tracers. 1. Models and their applicability. *J. Hydrol.* [https://doi.org/10.1016/0022-1694\(82\)90147-0](https://doi.org/10.1016/0022-1694(82)90147-0).
- Mashburn, S.L., Cope, C.C., Abbott, M.M., 2003. Aquifer characteristics, water availability, and water quality of the Quaternary aquifer, northeastern Oklahoma, 2001–2002, Vol. 3. US Department of the Interior, US Geological Survey.
- McDonnell, J.J., McGuire, K., Aggarwal, P., Beven, K.J., Biondi, D., Destouni, G., Dunn, S., James, A., Kirchner, J., Kraft, P., 2010. How old is streamwater? Open questions in catchment transit time conceptualization, modeling and analysis. *Hydrol. Process.* 24, 1745–1754. 24: 1745–1754.
- McGuire, K.J., McDonnell, J., 2006. A review and evaluation of catchment transit time modeling. *J. Hydrol.* 330 (3–4), 543–563.
- McGuire, K.J., McDonnell, J.J., Weiler, M., Kendall, C., McGlynn, B.L., Welker, J.M., Seibert, J., 2005. The role of topography on catchment-scale water residence time. *Water Resour. Res.* 41 (5) <https://doi.org/10.1029/2004WR003657>.
- McMurdie, P., Holmes, S., 2013. phyloseq: An R package for reproducible interactive analysis and graphics of microbiome census data. *PloS One* 8 (4), e61217.
- Monnier, S., Kinnard, C., 2017. Pluri-decadal (1955–2014) evolution of glacier-rock glacier transitional landforms in the central Andes of Chile (30–33° S). *Earth Surf. Dyn.* 5 (3).
- Morris, D.A., Johnson, A.I., 1967. Summary of hydrologic and physical properties of rock and soil materials, as analyzed by the hydrologic laboratory of the US Geological Survey, 1948–60. US Government Printing Office.
- Musselman, K.N., Clark, M.P., Liu, C., Ikeda, K., Rasmussen, R., 2017. Slower snowmelt in a warmer world. *Nat. Clim. Change* 7 (3), 214–219.
- Newman, B.D., Osenbrück, K., Aeschbach-Hertig, W., Kip Solomon, D., Cook, P., Różański, K., Kipfer, R., 2010. Dating of ‘young’ groundwaters using environmental tracers: advantages, applications, and research needs. *Isot. Environ. Health Stud.* 46 (3), 259–278. <https://doi.org/10.1080/10256016.2010.514339>.
- Ó Dochartaigh, B.É., MacDonald, A.M., Black, A.R., Everest, J., Wilson, P., Darling, W.G., Jones, L., Raines, M., 2019. Groundwater–glacier meltwater interaction in proglacial aquifers. *Hydrol. Earth Syst. Sci.* 23 (11), 4527–4539.
- Obu, J., 2021. How much of the earth’s surface is underlain by permafrost? *J. Geophys. Res.: Earth Surf.* 126 (5) e2021JF006123.
- Obu, J., Westermann, S., Kaab, A., Bartsch, A., 2019. Ground Temperature Map, 2000–2016, Andes, New Zealand and East African Plateau Permafrost. University of Oslo, PANGAEA. <https://doi.org/10.1594/PANGAEA.905512>.
- Ohlanders, N., Rodriguez, M., McPhee Torres, J., 2013. Stable water isotope variation in a Central Andean watershed dominated by glacier and snowmelt. *Hydrol. Earth Syst. Sci.*
- Oksanen, J., Blanchet, F.G., Friendly, M., Kindt, R., Legendre, P., McGlinn, D., Minchin, P.R., O’Hara, R.B., Simpson, G.L., & Solymos, P. (2019). *vegan: Community Ecology Package*. R package version 2.5–6. 2019.

- Parada, A.E., Needham, D.M., Fuhrman, J.A., 2016. Every base matters: assessing small subunit rRNA primers for marine microbiomes with mock communities, time series and global field samples. *Environ. Microbiol.* 18 (5), 1403–1414.
- Quast, C., Pruesse, E., Yilmaz, P., Gerken, J., Schweer, T., Yarza, P., Peplies, J., Glöckner, F.O., 2012. The SILVA ribosomal RNA gene database project: improved data processing and web-based tools. *Nucleic Acids Res.* 41 (D1), D590–D596.
- Ramírez, P.B., Fuentes-Alburquerque, S., Díez, B., Vargas, I., Bonilla, C.A., 2020. Soil microbial community responses to labile organic carbon fractions in relation to soil type and land use along a climate gradient. *Soil Biol. Biochem.* 141, 107692.
- Rodgers, P., Soulsby, C., Waldron, S., 2005. Stable isotope tracers as diagnostic tools in upscaling flow path understanding and residence time estimates in a mountainous mesoscale catchment. *Hydrolog. Process.: Int. J.* 19 (11), 2291–2307.
- Rodriguez, M., Ohlanders, N., McPhee, J., 2014. Estimating glacier and snowmelt contributions to stream flow in a Central Andes catchment in Chile using natural tracers. *Hydrolog. Earth Syst. Sci. Discuss.* 11 (7), 8949–8994.
- Rodriguez, M., Ohlanders, N., Pellicciotti, F., Williams, M.W., McPhee, J., 2016. Estimating runoff from a glaciated catchment using natural tracers in the semi-arid Andes cordillera. *Hydrolog. Process.* 30 (20), 3609–3626. <https://doi.org/10.1002/hyp.10973>.
- Rognes, T., Flouri, T., Nichols, B., Quince, C., Mahé, F., 2016. VSEARCH: a versatile open source tool for metagenomics. *PeerJ* 4, e2584.
- Rose, S., 2007. Utilization of decadal tritium variation for assessing the residence time of base flow. *Groundwater* 45 (3), 309–317.
- Ruiz Pereira, S., Veettil, B.K., 2019. Glacier decline in the Central Andes (33° S): Context and magnitude from satellite and historical data. *J. South Am. Earth Sci.* 102249.
- Ruiz Pereira, S., Marquardt, C., Beriain, E., Lambert, F., 2021. Permafrost evolution in a mountain catchment near Santiago de Chile. *J. South Am. Earth Sci.*, 103293.
- Saberi, L., McLaughlin, R.T., Ng, G.-H., Frenierre, J., La, Wickert, A.D., Baraer, M., Zhi, W., Li, L., Mark, B.G., 2019. Multi-scale temporal variability in meltwater contributions in a tropical glaciated watershed. *Hydrolog. Earth Syst. Sci.* 23 (1), 405–425.
- Saito, K., Trombotto Liudat, D., Yoshikawa, K., Mori, J., Sone, T., Marchenko, S., Romanovsky, V., Walsh, J., Hendricks, A., Bottega, E., 2016. Late quaternary permafrost distributions downscaled for South America: examinations of GCM-based maps with observations. *Permafrost. Periglac. Process.* 27 (1), 43–55.
- Sajjad, W., Ali, B., Bahadur, A., Ghimire, P.S., Kang, S., 2021. Bacterial diversity and communities structural dynamics in soil and meltwater runoff at the frontier of Baishui Glacier No. 1, China. *Microb. Ecol.* 81 (2), 370–384.
- Sakata, Y., Ikeda, R., 2013. Depth dependence and exponential models of permeability in alluvial-fan gravel deposits. *Hydrogeol. J.* 21 (4), 773–786.
- Slaymaker, O., 2009. Proglacial, Periglacial or Paraglacial?, 320. Special Publications, Geological Society, London, pp. 71–84.
- Somers, L.D., McKenzie, J.M., 2020. A review of groundwater in high mountain environments. *Wiley Interdiscip. Rev.: Water* 7 (6), e1475.
- Somers, L.D., McKenzie, J.M., Mark, B.G., Lagos, P., Ng, G.C., Wickert, A.D., Yarleque, C., Baraér, M., Silva, Y., 2019. Groundwater buffers decreasing glacier melt in an Andean watershed—But not forever. *Geophys. Res. Lett.* 46 (22), 13016–13026.
- Stewart, M.K., Morgenstern, U., McDonnell, J.J., 2010. Truncation of stream residence time: how the use of stable isotopes has skewed our concept of streamwater age and origin. *Hydrolog. Process.* 24 (12), 1646–1659. <https://doi.org/10.1002/hyp.7576>.
- Stewart, M.K., Morgenstern, U., Gusyev, M.A., Małoszewski, P., 2017. Aggregation effects on tritium-based mean transit times and young water fractions in spatially heterogeneous catchments and groundwater systems. *Hydrolog. Earth Syst. Sci.* 21 (9), 4615–4627. <https://doi.org/10.5194/hess-21-4615-2017>.
- Stewart, M.K., Morgenstern, U., Cartwright, I., 2021. Comment on “A comparison of catchment travel times and storage deduced from deuterium and tritium tracers using StorAge Selection functions” by Rodriguez et al.(2021). *Hydrolog. Earth Syst. Sci. Discuss.* 1–8.
- Szopińska, M., Szumińska, D., Polkowska, Ž., Machowiak, K., Lehmann, S., Chmiel, S., 2016. The chemistry of river-lake systems in the context of permafrost occurrence (Mongolia, Valley of the Lakes). Part I. Analysis of ion and trace metal concentrations. *Sediment. Geol.* 340, 74–83.
- Tapia Baldis, C., Trombotto Liudat, D., 2019. Rockslides and rock avalanches in the Central Andes of Argentina and their possible association with permafrost degradation. *Permafrost. Periglac. Process.* 30 (4), 330–347.
- Team, R.C. (2020). *R: a language and environment for statistical computing*. R Foundation for Statistical Computing website.
- Toohey, R.C., Herman-Mercer, N.M., Schuster, P.F., Mutter, E.A., Koch, J.C., 2016. Multidecadal increases in the Yukon River Basin of chemical fluxes as indicators of changing flowpaths, groundwater, and permafrost. *Geophys. Res. Lett.* 43 (23).
- Toubes-Rodrigo, M., Potgieter-Vermaak, S., Sen, R., Elliott, D.R., & Cook, S.J. (2017). Geomicrobiology of basal ice in a temperate glacier: implications for primary microbial production and export, elemental cycling and soil formation. *EGU General Assembly Conference Abstracts*, 519.
- Wagner, B.D., Grunwald, G.K., Zerbe, G.O., Mikulich-Gilbertson, S.K., Robertson, C.E., Zemanick, E.T., Harris, J.K., 2018. On the use of diversity measures in longitudinal sequencing studies of microbial communities. *Front. Microbiol.* Vol. 9, 1037.
- Wan, C., Gibson, J.J., Shen, S., Yi, Y., Yi, P., Yu, Z., 2019. Using stable isotopes paired with tritium analysis to assess thermokarst lake water balances in the Source Area of the Yellow River, northeastern Qinghai-Tibet Plateau, China. *Sci. Total Environ.* 689, 1276–1292.
- Wu, W.-Y., Lo, M.-H., Wada, Y., Famiglietti, J.S., Reager, J.T., Yeh, P.J.-F., Ducharme, A., Yang, Z.-L., 2020. Divergent effects of climate change on future groundwater availability in key mid-latitude aquifers. *Nat. Commun.* 11 (1), 1–9.
- Yi, P., Wan, C., Jin, H., Luo, D., Yang, Y., Wang, Q., Yu, Z., Aldahan, A., 2018. Hydrological insights from hydrogen and oxygen isotopes in Source Area of the Yellow River, east-northern part of Qinghai-Tibet Plateau. *J. Radioanal. Nucl. Chem.* 317 (1), 131–144. <https://doi.org/10.1007/s10967-018-5864-7>.
- Yu, C., Kamboj, S., Wang, C., Cheng, J.-J. 2015. Data Collection Handbook to Support Modeling Impacts of Radioactive Material in Soil and Building Structures. Argonne National Lab.(ANL), Argonne, IL (United States).
- Zech, M., Tuthorn, M., Detsch, F., Rozanski, K., Zech, R., Zöller, L., Zech, W., Glaser, B., 2013. A 220 ka terrestrial $\delta^{18}\text{O}$ and deuterium excess biomarker record from an eolian permafrost paleosol sequence, NE-Siberia. *Chem. Geol.* 360, 220–230.
- Zhong, Z.-P., Tian, F., Roux, S., Gazitúa, M.C., Solonenko, N.E., Li, Y.-F., Davis, M.E., Van Etten, J.L., Mosley-Thompson, E., Rich, V.I., Sullivan, M.B., Thompson, L.G., 2021. Glacier ice archives nearly 15,000-year-old microbes and phages. *Microbiome* 9 (1), 160. <https://doi.org/10.1186/s40168-021-01106-w>.